Proceedings of the ASME 2023
International Design Engineering Technical Conferences and
Computers and Information in Engineering Conference
IDETC-CIE2023

DETC2023-115235

August 20-23, 2023, Boston, Massachusetts

DYNAMIC MODELING AND ROUBUST TOUQUE CONTROL OF A DISCRETE VARIABLE STIFFNESS ACTUATOR

Ziqing Yu, Jiaming Fu, Bin Yao, George Chiu, Richard Voyles, Dongming Gan*

Purdue, West Lafayette, IN, *corresponding: dgan@purdue.edu

ABSTRACT

Collaborative robots, or cobots, have been developed as a solution to the growing need for robots that can work alongside humans safely and effectively. One emerging technology in robotics is the use of Discrete Variable Stiffness Actuators (DVSAs), which enable robots to adjust their stiffness in a fastdiscrete manner. This enables cobots to work in both low and high stiffness modes, allowing for safe collaboration with human workers or operation behind safety barriers. However, achieving good performance with different stiffness modes of DVSAs is a challenging problem. This paper proposes a method to provide force control of a DVSA by exploiting the dynamic model and the discrete stiffness levels. The two-mass dynamic model, a widely accepted model of flexible systems, is used to model and analyze the DVSA. The proposed method involves using Gain-scheduling and Deterministic Robust Control (DRC) controllers as modelbased control algorithms for the DVSA to achieve high-precision force control. We also conducted a comparison with the commonly used proportional integral derivative (PID) control algorithms. The paper presents a detailed analysis of the dynamic behavior of the DVSA and demonstrates the effectiveness of the proposed control algorithms through simulation with different scenario comparisons, even in the presence of external disturbances.

Keywords: DVSAs, Gain-scheduling, Deterministic Robust Control, two-mass dynamic model

1. INTRODUCTION

With the rapid development of technology [1-2], the use of robots designed to work alongside humans in shared workspaces is on the rise. Collaborative robots are capable of performing a diverse range of tasks, such as assembly, welding, packaging, and inspection, and are especially useful for tasks that are repetitive or hazardous to human workers. By introducing collaborative robots in manufacturing, the efficiency of robots can be fully utilized to compensate for the limitations of humans in terms of precision, strength, and durability, while retaining human intelligence and skills [3-5]. This approach allows for the optimization of the manufacturing process, leading to increased productivity, reduced costs, and improved safety for workers. The integration of collaborative robots has opened up new possibilities for the development of innovative manufacturing processes and products that were previously unattainable.

Safety of human/robot interaction is of utmost importance in collaborative robotics [6]. While the use of force sensors [7] to detect human presence is a common solution, it can be complicated and prone to errors. An alternative solution is to employ variable stiffness actuators (VSAs) at the joints of cobots. VSAs are designed based on the variable impedance actuation (VIA) method to improve torque bandwidth and reduce structure sizes [8–10]. Other VSAs can also adjust stiffness by changing the effective beam length to achieve continuous variable stiffness [11,12]. However, most continuous stiffness change methods result in bulk designs, slow stiffness change speed and undesired stiffness curves. This has led to the development of discrete variable stiffness actuators (DVSAs) [13-15] which are a type of actuators that can adjust stiffness in large discrete levels for representative application needs. DVSAs

offer a simpler and less complex solution for adjusting stiffness, which can improve the safety and efficiency of human/robot interaction [16].

One of the major functions of VSAs is their intrinsic force control capability through their compliance elements. Force control is widely used in modern control of collaborative robots. For example, force mode control was used in human assistive robots for natural assistance [17]. Several torque control methods have been proposed for two-mass systems connected with an elastic element, as described in previous studies [18-20]. Additionally, the control of variable stiffness actuators (VSAs) through force control is fundamentally a control of the deflections of the VSAs. These deflections are determined by the difference between the motor-side and load-side dynamics. As can be seen from its application scenarios, like assistive robots and robot arms that are physically co-operative with human operators, it requires a certain degree of accuracy and ability to have a good performance at different stiffness levels.

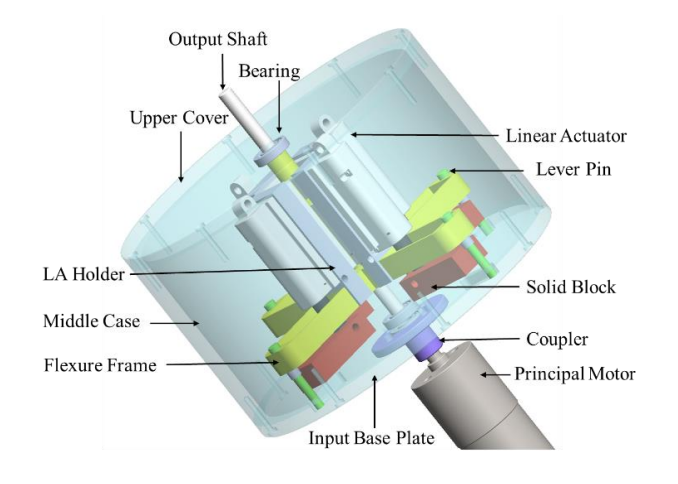
In a traditional Serial Elastic Actuator (SEA) two-mass system, the elasticity of the system's elastic element is typically determined through numerical calculations [21]. It was shown in this paper that the SEA can be modeled as the two-mass system, which also can include the environmental impedance. To control such systems, Disturbance Observers (DOB) have been used, which demonstrate effective attenuation of constant disturbances and slowly time-varying disturbances.

The DVSA two-mass system is similar to the SEA system, but with added complexity of multi-levels of stiffness. Therefore, the controller used for DVSA should be robust enough to handle the influence of different stiffness. In this paper, we developed a two-mass dynamic model of a new DVSA with four different stiffness levels and designed two torque control algorithms in comparison with the basic PID controller. The first method proposed for controlling the DVSA is the Gain-scheduling [22] controller, where the gain of the controller is selected based on the different stiffness levels. We prepare four different Proportional-Integral-Derivative (PID) gains to match the different stiffness levels. The second method, called Determined Robust Control (DRC) [26], is designed to maintain stability in the presence of external disturbances and changes in stiffness. It decouples torque control from the influence of dynamic changes on the load side, thereby theoretically guaranteeing stability and performance.

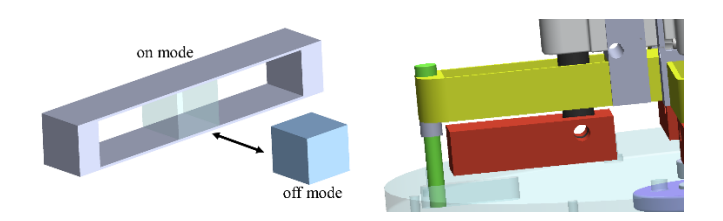
The paper is organized as follows: In Section 2, the mechanical design of a new DVSA is introduced. Theoretical models of the two-mass system are established in Section 3. Force control models based on Gain-scheduling and DRC are developed in Section 4. In Section 5, simulations are conducted to compare the performance of PID, Gain-scheduling, and DRC controllers in terms of step response and application scenarios. Conclusions make up Section 6.

2. MECHANICAL DESIGN

2.1 The DVSA Concept



(a) DVSA design



(b) variable stiffness beam (c) variable stiffness branch design

FIGURE 1: Mechanical design of the DVSA. It shows the mechanical design of the DVSA, which is based on a reconfigurable parallel beam design [24].

The newly developed DVSA is comprised of a principal motor, a stiffness adjustment mechanism and a stiffness transmission mechanism. A centrosymmetric four-branch frame is employed as the structure of the stiffness adjustment mechanism, as depicted in Fig. 1(a), to counterbalance forces and counteract parasitic motions. The compliant branch of each structure adopts a parallel-beam flexure, which reduces lateral bending compared to a single leaf spring and improves torque transmission efficiency. The DVSA achieves discrete variable stiffness by altering the cross-sectional area property, shown in Fig. 1(b). This is achieved by inserting or extracting a solid block into the cavity of the flexure to increase or decrease its stiffness. A compact low-power linear actuator (ACTUONIX PQ12-P), fixed on the flexure frame near the central shaft, is used to execute the function of stiffness change. A solid block is mounted on the stroke of the linear actuator, and the stroke passes through the cavity near the solid segment, shown in Fig.1(c). When the parallel beam bends, the middle part of the beam deforms significantly, and the deformation near the ends is relatively small. Consequently, the stroke does not come into contact with the beam and does not impede the deformation of the beam. When the stroke is extended, the solid block is pushed out of the cavity of the parallel beam, resulting in low stiffness and high compliance, called off mode. Conversely, when the

stroke is retracted, the solid block is pulled into the cavity, resulting in high stiffness and accuracy, called on mode.

The four branches can attain four different stiffness levels, enabling a maximum stiffness variation of 180.14 times. Fig. 2(a) illustrates the DVSA at maximum stiffness level, when all four branches are in on mode. Fig. 2(b) depicts the DVSA at minimum stiffness level, when all four branches are in off mode. The stroke extrusion or retraction process takes only 0.1 seconds, indicating that the stiffness can be altered swiftly. When the beam experiences significant deformation, the block cannot be inserted or pushed out smoothly, restricting the DVSA to achieving only offline variable stiffness.

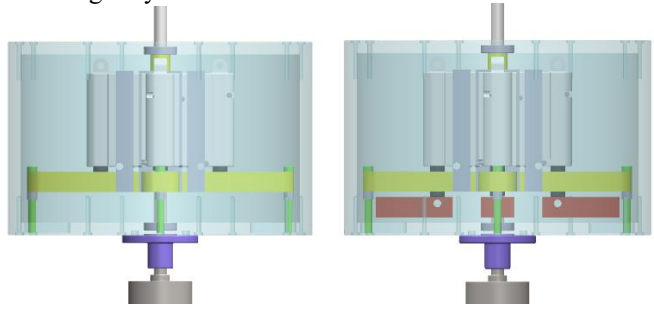


FIGURE 2: Discrete stiffness changes of the DVSA: (a) all branches are in 'on' mode (maximum stiffness); (b) all branches are in 'off' mode (minimum stiffness)

2.2 Stiffness transmission mechanism

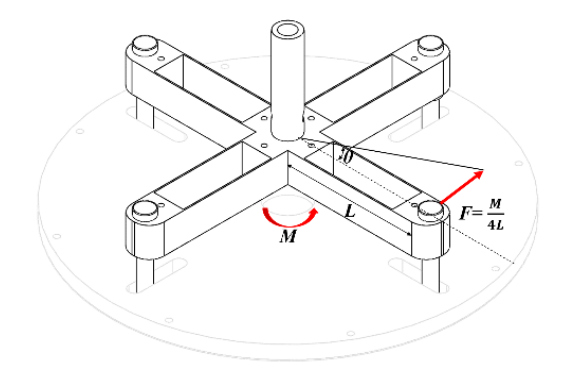


FIGURE 3: Schematic diagram of the load analysis

As shown in Fig. 3, the shaft of the main drive motor is linked to the input base plate located at the bottom of the DVSA via a coupler, generating a torque T that drives the entire housing to rotate. The torque T as equivalent to the moment M at the center of the plate, which propels the flexure frame to rotate through four lever pins. The effect of the moment M on the lever pins can be represented as a force F, which is equal to one-quarter M divided by the length of the force arm L, oriented perpendicular to L and tangent to the lever pins. The lever pins are inserted into a guide slot located above the plate, enabling them to move within the slot when the flexure frame is bent, ensuring that the force F is always perpendicular to L and tangent to the lever pin. The partial force along the L direction is small and can be disregarded. The flexure frame is fastened to the output shaft, and the output shaft is connected to the load.

According to the analytical model outlined in [13] for parallel beams, the total stiffness of the system K_{total} , can be computed as follows:

$$K_{total} = \sum_{i=1}^{n} K_i \tag{1}$$

In this case when *n*=4, which represents the number of branches in the flexure frame.

Table 1 elaborates the principal dimensional and performance parameters of the DVSA, which is used in the following study and can be customized as actual requirements.

Table 1. Main specifications of the DVSA

Parameters	Values	Units
Outer diameter of the DVSA	120	mm
Hight of the DVSA	75	mm
Effective length of the parallel beam	30	mm
Thickness of the parallel beam	0.8	mm
Width of the flexure frame	15	mm
Thickness of the flexure frame	8	mm
Range of stiffness variation	$3.61 \sim 650.31$	Nm/°
Range of deflection	0 ~ 11.46	0
Stiffness variation time	0.1	S
Young's modulus of the flexure frame (Al 6061)	69	GPa

3. ANALYSIS OF DVSA DYNAMICS FOR FORCE CONTROL

3.2 Modeling of the DVSA as a Two-Mass System

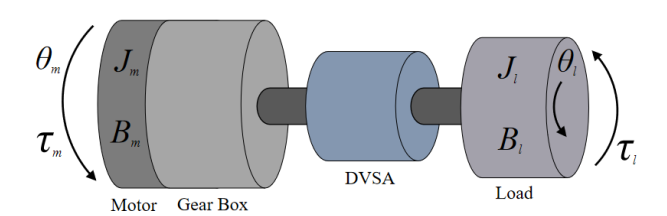


FIGURE 4: Dynamic model of the DVSA

As show in Fig. 4, the two system represent the motor-side and load-side models. J_l , J_m represent the inertial of load-side and motor-side and B_l , B_m are the viscous friction coefficient of the load side and motor side. N represents the reduction ration of the gear box. The variable stiffness mechanism connects two sides as elastic element where K stands for the elastic coefficient.

All the system is driven by a DC motor which can provide stable input τ_m And τ_l is the output of system we need to control.

$$J_l \ddot{\theta_l} + B_l \dot{\theta_l} = K(\frac{\theta_m}{N} - \theta_l) + d_l \tag{2}$$

$$J_n \ddot{\theta}_l + B_n \dot{\theta}_l + K_n \theta_l = K \left(\frac{\theta_m}{N} - \theta_l \right) + d_l \tag{3}$$

 $\ddot{\theta}_l$, $\dot{\theta}_l$, and θ_l represent the acceleration, velocity, and displacement of load-side, respectively. d_l is the disturbance in the motor-side like the friction and resistance. When considering environmental variables, the symbols J_n and B_n denote the inertial and viscous friction coefficients, respectively, of the load-side. And the difference between of displacement of the two sides shows the deformation of the elastic element which provides the force for the load-side.

To investigate interaction configurations of the system with environment, two different cases should be considered. In the free case, the environment parameters $J_e = 0$, $B_e = 0$, and $K_e = 0$. On the other hand, in the fully constrained case, the environmental parameters are set to $J_e = 0$, $B_e = 5B_l$, and $K_e = 200$ to simulate a stiff environment contact. Therefore, the inertial and viscous friction coefficient can be written as $J_n = J_e + J_l$ and $B_n = B_e + B_l$. This change of the environmental K parameters would introduce a meaningful model variation into the DVSA control system.

$$J_m \ddot{\theta}_m + B_m \dot{\theta}_m = K_m u + d_m \tag{4}$$

On the motor-side $\ddot{\theta}_m$, $\dot{\theta}_m$, and θ_m represent the acceleration, velocity, and displacement of load-side, respectively. d_m is the disturbance in the motor-side like the friction and resistance. The model Eq. (3), Eq. (4) are transformed to the strict feedback form with internal dynamics. To design the controller, we define that $x_1 = \theta_l$, $x_2 = \dot{\theta}_l$, $z_1 = \frac{\theta_m}{N} - \theta_l$ and $z_2 = \frac{\dot{\theta}_m}{N} - \dot{\theta}_l$, the dynamics of the DVSA torque control is modeled as:

$$\begin{cases} \dot{x}_{1} = x_{2} \\ \dot{x}_{2} = -\frac{K}{J_{n}}x_{1} - \frac{B_{n}}{J_{n}}x_{2} + \frac{d_{l}}{J_{n}} \\ \dot{z}_{1} = z_{2} \\ \theta_{0}\dot{z}_{2} = u - \theta_{1}z_{1} - \theta_{2}z_{2} + \theta_{3}x_{2} + \widetilde{\Delta} \\ y = z_{1} \end{cases}$$
 (5)

From Eq. (5), we can read the x_2 dynamics represents the equivalent load-side dynamics and z_2 dynamic represents the torque tracking dynamics by the relationship between torque and position difference. The parameters in this equation are dependent on the change of the stiffness and influence of environmental parameters. They can be written as:

$$\theta_0 = NJ_n, \ \theta_1 = \frac{1}{J_n} + NJ_m - NJ_n$$
 $\theta_2 = NB_n, \ \theta_1 = -NB_n + \frac{NB_nJ_m}{J_n}$ (6)

$$\widetilde{\Delta} = d_m + (\frac{NJ_m}{J_n} - 2)d_{mL}$$

4. TORQUE CONTROLLER DESIGN WITH ROBUST COMPENSATION

In this section, a torque control scheme for the DVSA is presented. To guarantee certain transient performance and final tracking accuracy, it needs to be robust enough to deal with the parametric uncertainties caused by change of the stiffness and influence of environmental parameters, disturbance of motorside and load-side and nonlinearities. Deterministic Robust Control is used to synthesize nonlinear feedback which overpowers all types of model uncertainty effects to achieve not only robust stability but also certain robust performance as well.

4.1 Gain-scheduling controller design

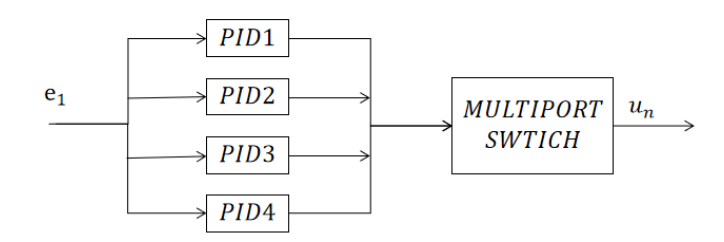


FIGURE 5: Gain-scheduling controller

PID controller is a widely used control strategy in industrial applications [23]. It is easy to operate but may not respond well to sudden or large setpoint changes. For our DVSA two-mass system, the PID controller is easy to implement and provides good control performance for a wide range of control applications with certain gain values. However, it suffers from the lack of adaptive re-tuning of its gains for systems with varying stiffness and uncertain environments, which may lead to instability in feedback control. Thus, a more adaptive control method, the Gain-scheduling control [22], is developed to provide different values of the PID gains for different levels of stiffness. Comparing with the traditional PID controller, the Gain-scheduling controller improves the control performance and robustness and guarantees the stability of the control system. Eq. (7) defines the tracking error in the gain scheduling design, and u_n is the Gain-scheduling control term.

$$e_1 = z_1 - y_d \tag{7}$$

$$u_n = K_{mn}e_1(t) + K_{in}\int e_1(t) + K_{dn}\dot{e_1}(t)$$
 (8)

With the four different stiffness levels at n = 1, 2, 3, 4, four different sets of parameters $\{K_{pn}, K_{in}, K_{dn} \text{ are going to be designed for corresponding stiffness.}\}$

4.2 Determined robust controller design

Deterministic robust control (DRC) [26] utilizes precisely known system characteristics and the known upper bound of

model uncertainties in sliding mode control (SMC) [25]. In Fig. 5, k_2 represents the linear stabilizing feedback and u_{s2} represents the nonlinear robust feedback.

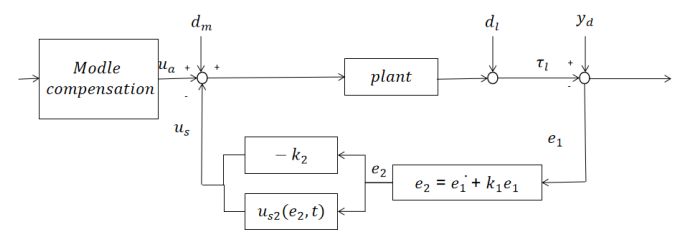


FIGURE 6: DRC control method

The tracking error can be defined as $e_1 = z_1 - y_d$, and $e_2 = \dot{e_1} + k_1 e_1 = z_2 - z_{2d}$. In this equation we can find that the e_2 will be small or converge to zero when k_1 is a positive feedback gain. From $G_Z(s) = \frac{z_1(s)}{z_2(s)} = \frac{1}{s+k_1}$, it can be known that e_1 will also be small or converge to zero.

$$\begin{array}{l} \theta \in \Omega_{\theta} \triangleq \{\theta \colon \quad \theta_{min} < \theta < \theta_{max} \} \\ \Delta \in \Omega_{\triangleq} \{\Delta \colon \quad | \Delta(x,t) | \leq \delta(x,t) \} \end{array} \tag{9}$$

As the uncertain parameters, we can get the minimum value $\theta_{min} = [\theta_{0\min}, \theta_{1\min}, \theta_{2\min}, \theta_{3\min}]^T$ and maximum value $\theta_{min} = [\theta_{0\max}, \theta_{1\max}, \theta_{2\max}, \theta_{3\max}]^T$, $\delta(x, t)$ is the known bound of the disturbance. Due to a certain bound Eq. (9) of the parameter and disturbance, the control input can be written

$$u = u_a + u_s \tag{10}$$

And from

$$\theta_0 \dot{e}_2 = u + \boldsymbol{\psi}^T \boldsymbol{\theta} + \widetilde{\Delta} \tag{11}$$

 u_a can be defined as:

$$u_a = -\boldsymbol{\psi}^T \widehat{\boldsymbol{\theta}} \tag{12}$$

 $\theta = [\theta_0, \theta_1, \theta_2, \theta_3]^T$, and the regression which depends on the actual states z_1, z_2 can be written as $\psi = [-\dot{z}_2, -z_1, -z_2, x_1, 1]^T$, u_s is a robust control term as in Fig. 5 having the following forms:

$$u_{s} = u_{s1} + u_{s2} \tag{13}$$

$$u_s = u_{s1} + u_{s2}$$
 (13)
$$u_{s1} = -k_2 e_2$$
 (14)

 u_{s1} is feedback to stabilize the nominal system and $k_2 >$ 0 is a positive gain.

After defining each value of u_a from Eq. (12) and in u_s from Eq. (13-14), we can have Eq. (15) from subtract u_a and u_s from Eq. (11):

$$\dot{e_2} + k_2 e_2 = u_{s2} - \left[\varphi(x)^T \tilde{\theta}_o - \Delta(x, t)\right] \tag{15}$$

The $\widetilde{m{ heta}}_o$ is defined as $\widetilde{m{ heta}}_o = \widehat{m{ heta}}_o - m{ heta}$. The left side of Eq. (15) represents the stable nominal closed loop dynamics. The terms inside the brackets in Eq. (15) represent the effects of all model uncertainties. Though these terms are unknown, u_{s2} are bounded above with some known functions h(x,t):

$$|\varphi(x)^T \tilde{\theta}_o - \Delta(x, t)| \le h(x, t)$$

$$h(x, t) = ||\theta_{\text{max}} - \theta_{\text{min}}|| ||\psi|| + \delta_{\Delta}$$
(16)

$$h(x,t) = \| \theta_{\text{max}} - \theta_{\text{min}} \| \| \psi \| + \delta_{\Delta}$$
 (17)

With the SMC law, all signals in the system Eq. (5) are bounded and the output tracking error e_2 exponentially converges to zero. u_{s2} is a nonlinear robust performance feedback term to improve the robust performance and decrease the influence of parameter uncertainties. Therefore, as in DRC, if robust feedback u_{s2} can be synthesized so that the following conditions should be satisfied:

i.
$$e_2(u_{s2} - \psi^T \tilde{\theta} + \tilde{\Delta}) \le \varepsilon$$

ii. $u_{s2} e_2 \le 0$ (18)

 ε is a designed parameter that can be arbitrarily small. u_{s2} can be written as smooth example to satisfy i. and ii. which can be designed as:

$$u_{s2} = -\frac{1}{4s}h(x,t)^2z\tag{19}$$

5. RESULT

In this section, a gain-scheduling controller and a determined robust controller are used for the DVSA two-mass system to compare the robust performance in comparison with a basic PID controller. This verifies the robust performance with parameter uncertainty especially the change of stiffness and disturbances. Two performance cases are simulated. The first simulation will show the step response of different methods at the four different levels of stiffness. Considering a potential application scenario of the DVSA, the second simulation is about torque control of the model with stiffness changing during the

Table 2. are the parameters being used in the simulation. By calculating the Range of stiffness variation times Range of deflection, we can get 4 levels of stiffness in the DVSA. Assumed in the constrained case, the environmental parameters are set to $J_n = 0$, Bn = 5Bl, and $k_n = 10k$.

Table 2. Dynamic parameters of the DVSA

Parameters	Values	Units
Inertial of load-side J_m	5.2500e-6	kg·m2
Inertial of motor-side J_l	0.0225	kg·m2
viscous friction coefficient of load-side B_l	4.5356e-6	Nm·s/rad
viscous friction coefficient of motor-side B_m	0.4697	Nm·s/rad
Reduction ratio N	20	

5.1 Step response of the proposed controllers

The step response setup involves applying a sudden change in force from zero to 1N on a system and observing how the system responds to this change. The total duration of the step response setup is typically 1 second, during which time the system's response is recorded. For this setup, there are four different stiffness levels that can be tested. Each level represents a different level of resistance to the applied force and can be adjusted by changing the properties of the system. To simulate the response of the system to the applied force, three different controllers can be used: proportional-integral-derivative (PID), gain scheduling, and dynamic recurrent control (DRC).

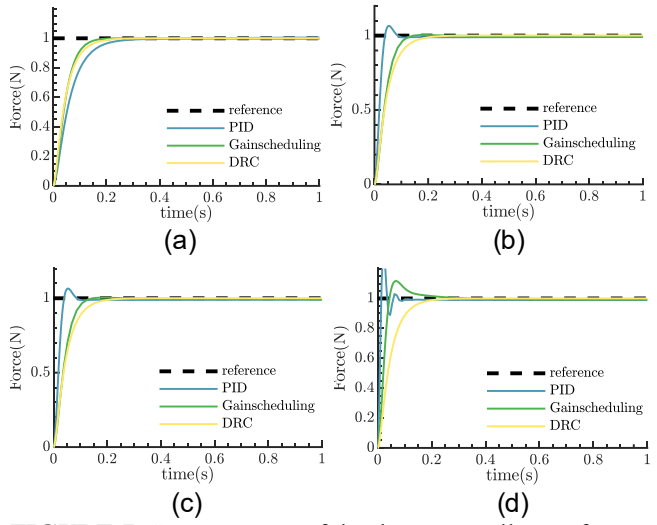


FIGURE 7: Step response of the three controllers at four different stiffness levels of the DVSA

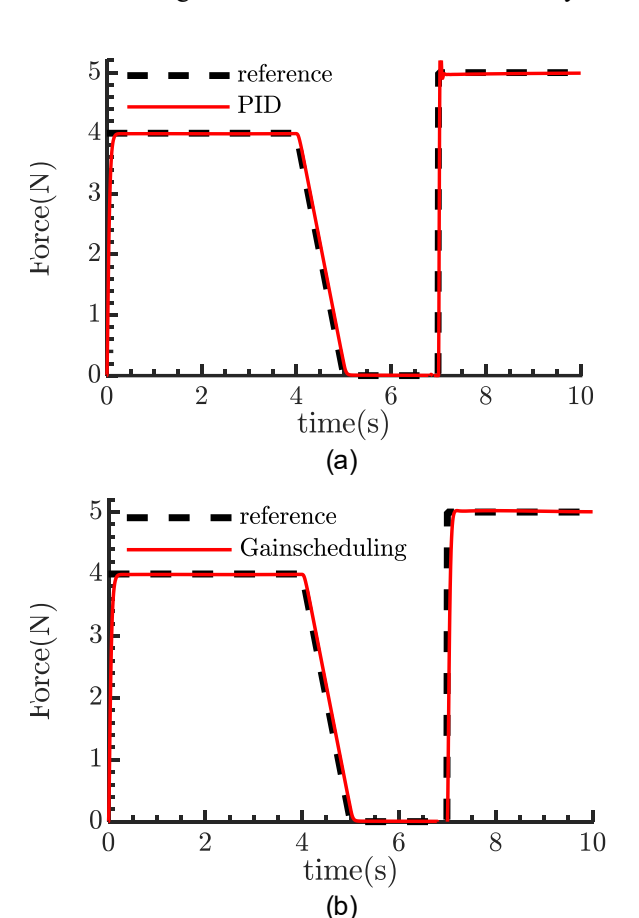
As shown in Fig. 7, a comparison is made between the step response of the PID, Gain-scheduling, and DRC controllers. Fig. 6(a) shows the step response in the first stiffness mode, which has the lowest stiffness. It is observed that the system with Gain-scheduling has the minimum settling time of t=0.215s, while the system with PID controller has the maximum settling time of t=0.455s. Moreover, the PID control system exhibits $10\%\sim20\%$ overshooting in other levels of stiffness due to its fixed PID gain. In contrast, the Gain-scheduling controller has less overshooting than the PID controller due to its adjustable PID gain. The DRC controller also provides a fast response, and

the settling time is close to that of the Gain-scheduling control system. The biggest advantage of DRC is that it eliminates overshoot in the system.

5.2 Application scenarios

The application setup involves a step response test where the system is subjected to two different force changes, one from zero to 4N and another from zero to 5N. The test is conducted over a duration of 10 seconds, with the initial force change occurring at t=0s and the second force change starting from t=7s. In addition to the step response test, there is a linear trajectory tracking test from t=4s to t=5s, during which time the system is expected to track a linear trajectory from 4N to zero. Finally, at t=6.8s, there is a change in stiffness level, which will affect the response of the system to any further force change.

Fig. 8 depicts the force control simulation results of the DVSA system when switching from low stiffness mode to high stiffness mode with varying force levels. In (a), the PID controller exhibits significant steady-state error and overshooting, indicating its poor performance in response to stiffness changes. Conversely, both the Gain-scheduling and DRC controllers show better performance, with the Gain-scheduling controller having the shortest settling time and the DRC controller having no overshoot. These results demonstrate the effectiveness of the proposed controllers in handling the stiffness changes and force control of the DVSA system.



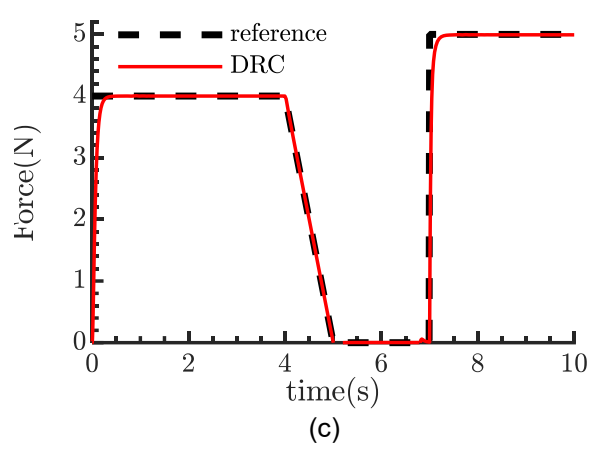


FIGURE 8: Trajectory tracking of application scenario.

6. Conclusions

This paper developed a new DVSA concept and its design with dynamics. Based on this, two control schemes were designed and compared with traditional PID controller for torque control with uncertainty considerations for potential cobot application scenarios. In conclusion, while PID controllers are easy to operate, they suffer from the lack of adaptive re-tuning of their gains for systems with varying stiffness and uncertain environments. Gain-scheduling and DRC controllers provide better control performance and robustness for DVSA systems, with Gain-scheduling having the minimum settling time and DRC being more stable and freer of overshooting. However, in future experiments, other factors such as uncertainty of parameters and environment should be considered, and a better controller with adaptive features should be explored.

ACKNOWLEDGMENT

This work is supported by the National Science Foundation (NSF) grant under CMMI-2131711

REFERENCES

- [1] Wang, Y., Li, B., Yan, F., & Chen, B. (2019). Practical adaptive fractional-order nonsingular terminal sliding mode control for a cable-driven manipulator. International Journal of Robust and Nonlinear Control, 29(5), 1396–1417.
- [2] Wang, Y., Yan, F., Chen, J., Ju, F., & Chen, B. (2019). A New Adaptive Time-Delay Control Scheme for Cable-Driven Manipulators. IEEE Transactions on Industrial Informatics, 15(6), 3469–3481.
- [3] Pearce, M., Mutlu, B., Shah, J. A., & Radwin, R. G. (2018). Optimizing Makespan and Ergonomics in Integrating Collaborative Robots Into Manufacturing Processes. IEEE Transactions on Automation Science and Engineering, 15(4), 1772–1784.
- [4] Schou, C., Andersen, R. S., Chrysostomou, D., Bøgh, S., & Madsen, O. (2018). Skill-based instruction of collaborative robots in industrial settings. Robotics and

- Computer-Integrated Manufacturing, 53, 72–80.
- [5] Brito, T., Queiroz, J., Piardi, L., Fernandes, L. M., Lima, J. L. F. C., & Leitão, P. (2020). A Machine Learning Approach for Collaborative Robot Smart Manufacturing Inspection for Quality Control Systems. Procedia Manufacturing, 51, 11–18.
- [6] Gan, D., Tsagarakis, N. G., Dai, J. S., Caldwell, D. G., & Seneviratne, L. (2013). Stiffness Design for a Spatial Three Degrees of Freedom Serial Compliant Manipulator Based on Impact Configuration Decomposition. Journal of Mechanisms and Robotics.
- [7] Voyles, R. M., Morrow, J., & Khosla, P. K. (1997). The Shape From Motion Approach to Rapid and Precise Force/Torque Sensor Calibration. Journal of Dynamic Systems Measurement and Control-Transactions of the Asme, 119(2), 229–235.
- [8] Liu, L., Leonhardt, S., Ngo, C., & Misgeld, B. J. E. (2020). Impedance-Controlled Variable Stiffness Actuator for Lower Limb Robot Applications. IEEE Transactions on Automation Science and Engineering, 17(2), 991–1004.
- [9] Schiavi, R., Grioli, G., Sen, S., & Bicchi, A. (2008). VSA-II: a Novel Prototype of Variable Stiffness Actuator for Safe and Performing Robots Interacting with Humans. International Conference on Robotics and Automation.
- [10] Zhu, Y., Wu, Q., Chen, B., Xu, D., & Ziyan, S. (2021). Design and Evaluation of a Novel Torque-Controllable Variable Stiffness Actuator With Reconfigurability. IEEE-ASME Transactions on Mechatronics, 27(1), 292–303.
- [11] Choi, J., Hong, S., Lee, W., Kang, S., & Kim, M. (2011). A Robot Joint With Variable Stiffness Using Leaf Springs. IEEE Transactions on Robotics, 27(2), 229–238.
- [12] Yapeng, X., Guo, K., Sun, J., & Li, J. (2021). Design, modeling and control of a reconfigurable variable stiffness actuator. Mechanical Systems and Signal Processing, 160, 107883.
- [13] Fu, J., Yu, Z., Lin, H., Zheng, L., & Gan, D. (2023). A Novel Variable Stiffness Compliant Robotic Link Based on Discrete Variable Stiffness Units for Safe Human-Robot Interaction. Journal of Mechanisms and Robotics, 1-25.
- [14] Hussain, I., Albalasie, A., Awad, M. I., Tamizi, K., Niu, Z., Seneviratne, L., & Gan, D. (2021). Design and control of a discrete variable stiffness actuator with instant stiffness switch for safe human-robot interaction. IEEE Access, 9, 118215-118231.
- [15] Awad, Mohammad I., Irfan Hussain, Dongming Gan, Ali Az-zu'bi, Cesare Stefanini, Kinda Khalaf, Yahya Zweiri, Tarek Taha, Jorge Dias, and Lakmal Seneviratne. "Passive Discrete Variable Stiffness Joint (pDVSJ-II): modeling, design, characterization, and testing toward passive haptic interface." Journal of Mechanisms and Robotics 11, no. 1 (2019): 011005.
- [16] Voyles, R. M., & Khosla, P. K. (1995). Tactile gestures for human/robot interaction. Intelligent Robots and Systems.
- [17] Oh, S., Baek, E., Song, S., Amirat, Y., Jeon, D., & Kong, K.

- (2015). A generalized control framework of assistive controllers and its application to lower limb exoskeletons. Robotics and Autonomous Systems, 73, 68–77.
- [18] Vallery, H., Ekkelenkamp, R., Van Der Kooij, H., & Buss, M. (2007). Passive and accurate torque control of series elastic actuators. Intelligent Robots and Systems.
- [19] Kong, K., Bae, J., & Tomizuka, M. (2009). Control of Rotary Series Elastic Actuator for Ideal Force-Mode Actuation in Human–Robot Interaction Applications. IEEE-ASME Transactions on Mechatronics, 14(1), 105– 118
- [20] Losey, D. P., Erwin, A., McDonald, C. M., Sergi, F., & O'Malley, M. K. (2016). A Time-Domain Approach to Control of Series Elastic Actuators: Adaptive Torque and Passivity-Based Impedance Control. IEEE-ASME Transactions on Mechatronics, 21(4), 2085–2096.
- [21] Oh, S., & Kong, K. (2017). High-Precision Robust Force Control of a Series Elastic Actuator. IEEE-ASME Transactions on Mechatronics, 22(1), 71–80.
- [22] L. Liu, S. Leonhardt, B. J. Misgeld, Experimental validation of a torque-controlled variable stiffness actuator tuned by gain scheduling, IEEE/ASME Transactions on Mechatronics 23 (5) (2018) 2109–2120.
- [23] Panda, R. C. (2012). Introduction to PID Controllers: Theory, Tuning and Application to Frontier Areas.
- [24] Fu, J., & Gan, D. (2021, August). A Reconfigurable Variable-Stiffness Parallel Beam for Compliant Robotic Mechanisms Towards Safe Human Interaction. In International Design Engineering Technical Conferences and Computers and Information in Engineering Conference (Vol. 85444, p. V08AT08A020). American Society of Mechanical Engineers.
- [25] Utkin, V. I. (1977). Variable structure systems with sliding modes. IEEE Transactions on Automatic Control, 22(2), 212–222.
- [26] Yao, B. (1996). Adaptive Robust Control of Nonlinear Systems with Application to Control of Mechanical Systems.